ORGANOMETALLICS
Article
pubs.acs.org/Organometallics

Photochemical Reaction of $Cp^*Ir(CO)_2$ with C_6F_5X (X = CN, F): Formation of Diiridium(II) Complexes

Kar Hang Garvin Mak,[†] Pek Ke Chan,[†] Wai Yip Fan,*[,†] Rakesh Ganguly,[‡] and Weng Kee Leong*[,‡]

[†]Department of Chemistry, National University of Singapore, 3 Science Drive 3, Singapore 117543
[‡]Division of Chemistry and Biological Chemistry, Nanyang Technological University, 21 Nanyang Link, Singapore 637371

Supporting Information

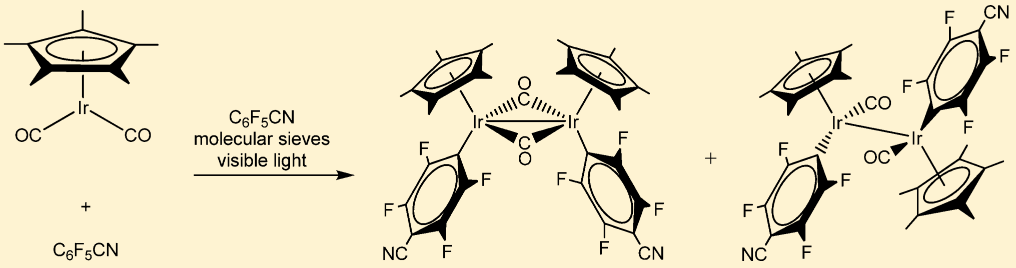

ABSTRACT: Visible light irradiation of $Cp^*Ir(CO)_2$ (**1**) in pentafluorobenzontrile resulted in the formation of the two isomeric diiridium(II) complexes $[Cp^*Ir(\mu\text{-}CO)(C_6F_4CN)]_2$ (**3**) and $[Cp^*Ir(CO)(C_6F_4CN)]_2$ (**4**), while the analogous reaction of **1** in hexafluorobenzene to give $[Cp^*Ir(\mu\text{-}CO)(C_6F_5)]_2$ (**3a**) required UV irradiation. Complex **4** isomerizes to **3** under visible light irradiation. A reaction pathway to **4** involving aromatic nucleophilic substitution has been proposed on the basis of experimental and computational data. The isomerization of **4** to **3** is believed to proceed via a radical species resulting from homolytic fission of the Ir−Ir bond.

INTRODUCTION

Iridium complexes generally have the oxidation states +1 and +3; Ir(II) complexes are uncommon, and those containing diiridium(II) are rarer still. In the reported examples, they are typically synthesized via oxidative addition of a substrate across the two iridium centers of a diiridium(I) species, and the resulting iridium(II) atoms are bridged by a ligand such as acetato, sulfido, sulfonylamido, or pyrazolato.[1−4] To date, there are only five known examples of diiridium(II) complexes containing no bridging ligands across the Ir−Ir bond, three of which contain large chelating ligands that seemingly stabilize the iridium(II) centers;[5−7] the fourth contains a chelating ligand that is apparently too bulky to bridge the metal centers,[8] and the fifth was synthesized via deprotonation of a bridged cationic dimeric species (Figure 1).[9]

Sometime ago, we reported that the reaction of $Cp^*Ir(CO)_2$ (**1**) with pentafluorobenzonitrile in the presence of water gave the metallocarboxylic acid species $Cp^*Ir(CO)(COOH)(C_6F_4CN)$ (**2**),[10] and a reaction pathway based on the nucleophilicity of **1**,[11] and the susceptibility of perfluorinated aromatic rings toward nucleophilic aromatic substitution,[12] was proposed (Scheme 1). Our earlier attempts at trapping the intermediate **A** were unsuccessful, which we presumed may be due to its susceptibility to hydrolysis. Under scrupulously dry conditions, however, we observed an unusual reaction leading to the formation of diiridium(II) complexes, which we wish to report here.

RESULTS AND DISCUSSION

The reaction of **1** in dry C_6F_5CN (scrupulously predried or in the presence of molecular sieves) under irradiation with a tungsten lamp (or more slowly under ambient light) gave a dark red suspension. Spectroscopic analysis indicated the presence of one major product, the diiridium(II) species $[Cp^*Ir(\mu\text{-}CO)(C_6F_4CN)]_2$ (**3**) and the minor isomer **4**; the yield of the latter could be increased by shortening the reaction time (Scheme 2). The two isomers decomposed on silica and could not be separated by fractional crystallization, but fractional crystallization afforded diffraction-quality crystals of both. In the presence of even adventitious moisture, complex **2** was obtained quantitatively instead.

In contrast, while **1** reacted with C_6F_5CN and water under ambient conditions to yield the metallocarboxylic acid **2**, there was no analogous reaction with C_6F_6. Complex **1** did react with C_6F_6 (10 mg/mL), however, under UV irradiation to give $Cp^*Ir(CO)(\eta^2\text{-}C_6F_6)$ (**5**) and $[Cp^*Ir(CO)(C_6F_5)]_2$ (**3a**) in a 5/1 ratio; a similar UV irradiation of **1** in C_6F_5CN gave an intractable mixture. Both **3a** and **5** have also been characterized by spectroscopy and by single-crystal X-ray crystallographic studies (Scheme 3). These products were also unstable on silica gel. Irradiation of a more dilute solution (4.4 mg/mL) gave only **5**, and prolonging the irradiation caused precipitation of a tan solid which contained a mixture of unidentified products. Heating the reaction mixture containing **1** and **5** at 80 °C also

Received: November 6, 2012
Published: February 6, 2013

dx.doi.org/10.1021/om301055h | *Organometallics* 2013, 32, 1053−1059

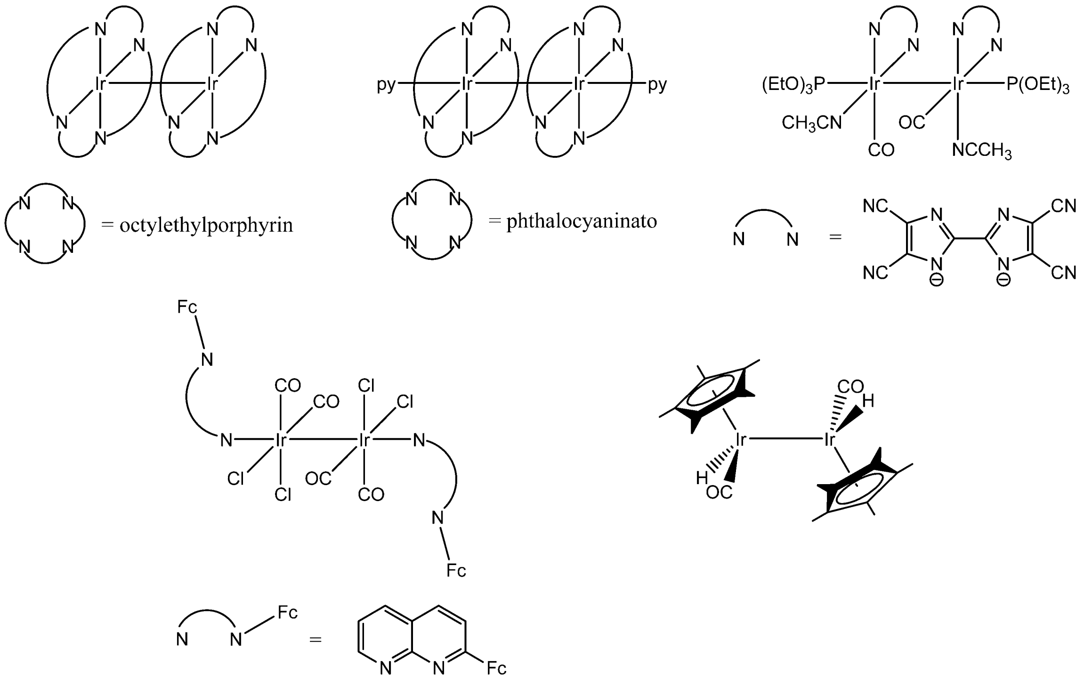

Figure 1. The only five known diiridium(II) complexes without a ligand bridging the Ir−Ir bond.

Scheme 1

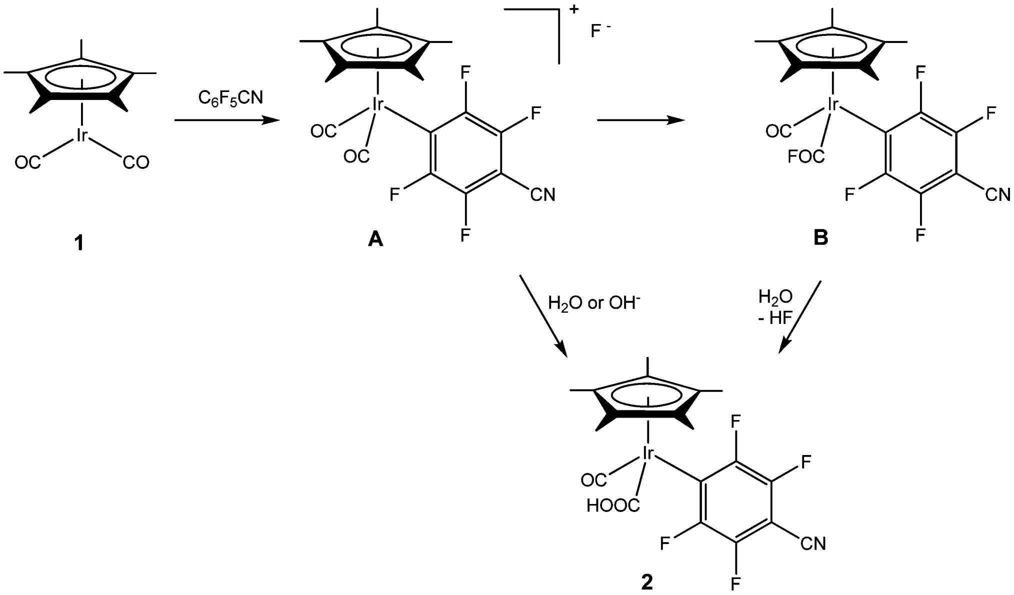

Scheme 2

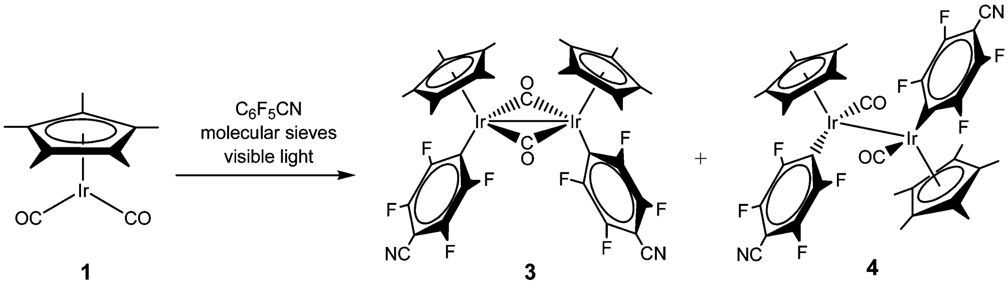

did not result in the formation of **3a**. These results suggested that **5** was unlikely to be the precursor to **3a**.

The decarbonylation of **1** under UV photoexcitation to form Cp*Ir(CO) (**1***)[13] has been well studied in relation to C−H

Scheme 3

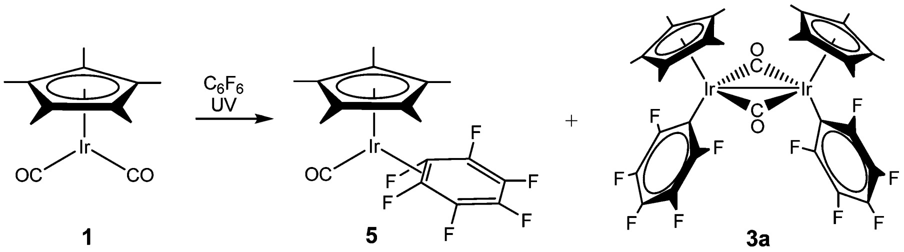

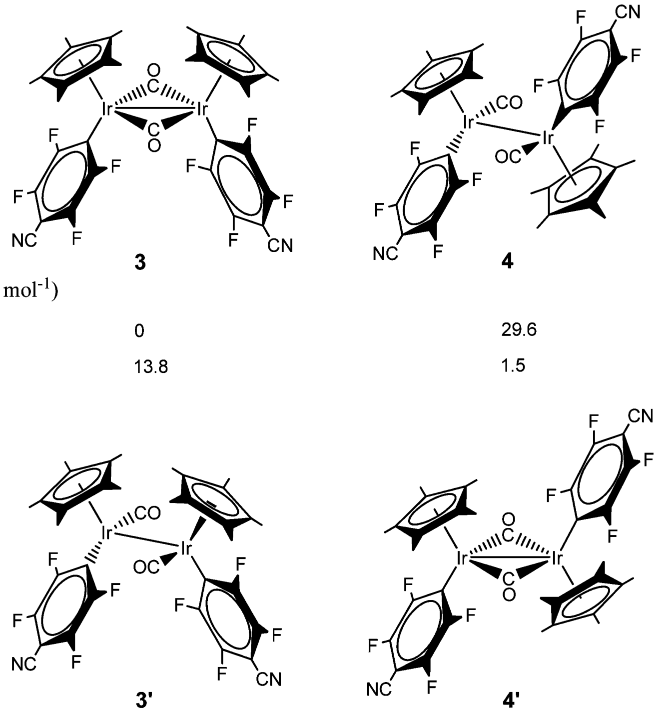

Relative energy (kJ mol^{-1})

	3	4
Solvated	0	29.6
Gas phase	13.8	1.5

	3'	4'
Solvated	8.4	28.0
Gas phase	24.3	0

Figure 2. Relative energies of **3** and **4** and their hypothetical isomers **3′** and **4′**.

bond activation[13−15] and was thus a possible precursor to **3a** and **5**. However, the fact that the UV−vis spectrum of **1** showed that a strong absorption band at 297 nm but absorbed poorly in the 350−500 nm (visible) region suggested that **1*** was unlikely to be responsible for the formation of **3** and **4** from C_6F_5CN. This difference in reactivity may be attributed to the increased susceptiblility to nucleophilic attack of C_6F_5CN in comparison to C_6F_6; the latter could only react with the highly reactive 16e species **1*** (to form **5**) or a UV-photoexcited **1** having increased nucleophilicity (to eventually form **3a**).[16]

Conversion of 4 to 3. NMR analyses showed that, with increasing irradiation time, the amount of unreacted **1** and **4** decreased relative to **3** until only the latter remained, suggesting that **4** converted irreversibly to **3** upon visible light irradiation. Synchronous opening of the two bridging carbonyls does not result in any change of the relative stereochemistry about the two iridium centers. The conversion of **4** to **3** must therefore involve cleavage of the Ir−Ir bond. Homolytic cleavage of the Ir−Ir bond to give the radical species $[Cp^*Ir(CO)(C_6F_4CN)]^\bullet$ (**C**) rather than a $[Cp^*Ir(CO)(C_6F_4CN)]^+[Cp^*Ir(CO)(C_6F_4CN)]^-$ ion pair was supported by the observation that **3** reacted quantitatively in the presence of visible light with $CHCl_3$ to form $Cp^*Ir(CO)(C_6F_4CN)(Cl)$ (**6**). The reaction failed to proceed in the absence of visible light irradiation, and a species such as $Cp^*Ir(CO)(C_6F_4CN)(CHCl_2)$, which may be expected from heterolytic cleavage of the Ir−Ir bond, was not observed.

The Gibbs free energies for **3** and **4** and for their respective stereoisomers **3′** and **4′** were computed (Figure 2). Compound **3** was computed to be 29.6 kJ/mol higher in energy than **4** in the gas phase, but the situation was reversed on solvation; it was 12.3 kJ/mol lower in energy in C_6F_5CN. This can be rationalized by the high polarity of **3** (19.6 D) and low polarity of **4** (0.0024 D) and accounted for the reason **3** was the major product in the reaction and why it was energetically favored in a polar environment; irradiation of a solution of **1** in a less polar mixture of C_6F_5CN and C_6F_6 (1/1, v/v) for 24 h gave a 9/1 mixture of **3** and **4**. The computed energies suggested that **4** first splits homolytically into two $[Cp^*Ir(CO)(C_6F_4CN)]^\bullet$ radicals, which would recombine, effectively with rotation of one of them about the Cp*−Ir axis, to generate **3′** but subsequent bridging of the Ir−Ir bond by the CO ligands to **3** was favored.

Scheme 4

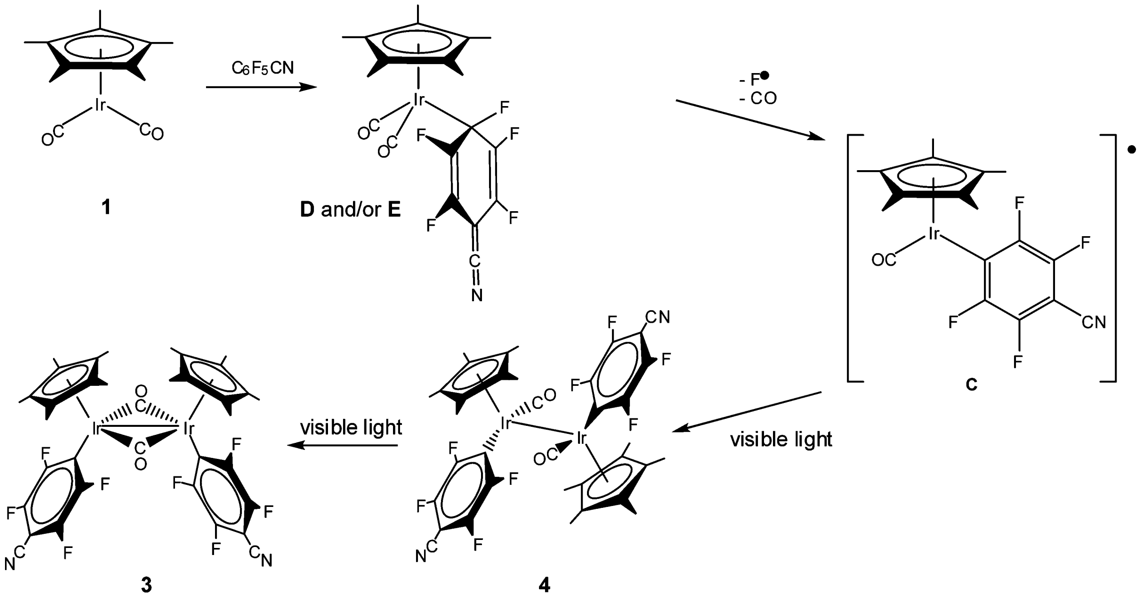

Mechanistic Investigations. The most likely reaction pathway by which **3** and **4** were formed was via reductive coupling of the acyl fluoride intermediate **B** with the elimination of oxalyl fluoride, either directly or via some other intermediate(s). However, our attempts to detect oxalyl fluoride or its hydrolysis product, oxalic acid, were unsuccessful. The reaction of **1** with C_6F_5CN (and molecular sieves) in the dark showed ~90% conversion after 24 h. The IR spectrum did not contain any absorption peak indicative of a −COF group, nor was there any resonance at around −53 ppm in the ^{19}F NMR spectrum, which would have been indicative of a −COF group attached to an Ir(III) center.[17] These ruled out the presence of **B**, but the spectroscopic data were assignable to a mixture of two unknown compounds **D** and **E**, in a 5/2 ratio. Variable-temperature ^{19}F NMR experiments showed no evidence of exchange between their signals, suggesting that they were separate species.

Both **D** and **E** were converted quantitatively to **6** upon standing in chloroform over an extended period of time and, upon visible light irradiation in C_6F_5CN, completely converted to **3** after 24 h. Freshly prepared **3** in C_6F_5CN showed no reaction upon stirring in complete darkness for 24 h. These observations indicated that **D** and **E** were precursors to **3**. Although we have not been able to assign definitive identities to them, we propose that they may be zwitterionic Meisenheimer-type complexes of the formula $Cp^*Ir(CO)_2(CFC_5F_4CN)$, from which loss of a CO and light-activated dissociation of a fluorine atom would lead to **C** (Scheme 4). We have studied the formation of such a complex computationally and found that the Gibbs free energy for its formation from **1** and C_6F_5CN was $+83$ kJ mol^{-1}.

Crystallographic Discussion. The X-ray crystal structures of **3**, **3a**, **4**, and **5** have all been determined; the ORTEP plots for **3** and **4** are shown in Figure 3. There are two crystallographically independent molecules found in the crystals of **3** and **3a**; a common atomic numbering scheme and selected bond parameters are given in Table 1. The molecular structures of **3** and **3a** are essentially the same; the perfluoroaryl rings are oriented perpendicular to the plane defined by the bridging carbonyls and are eclipsed and parallel to each other.

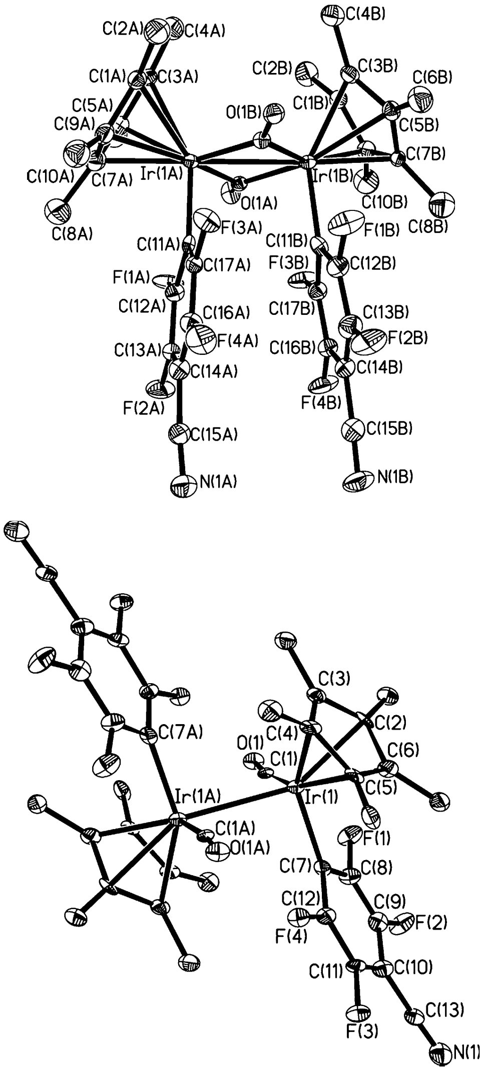

Figure 3. ORTEP plots of one of the crystallographically independent molecules of **3** (top) and **4** (bottom). Thermal ellipsoids are drawn at the 50% probability level. Hydrogen atoms have been omitted for clarity.

Table 1. Common Atomic Numbering Scheme and Selected Bond Parameters for 3 and 3a

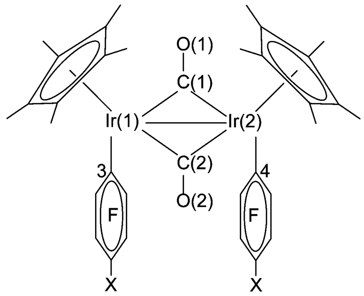

	3 (X = CN)		**3a** (X = F)	
param[a]	molecule A	molecule B	molecule A	molecule B
Ir(1)−Ir(2)	2.7655(5)	2.7485(5)	2.7576(8)	2.7583(8)
Ir(1)−C(1)	2.059(14)	2.049(11)	2.008(14)	2.040(14)
Ir(1)−C(2)	2.024(11)	2.049(11)	2.034(13)	2.014(14)
Ir(2)−C(1)	2.024(11)	2.027(11)	2.028(14)	2.001(14)
Ir(2)−C(2)	2.050(10)	2.017(11)	2.011(14)	2.035(13)
Ir(1)−C(3)	2.025(9)	2.046(14)	2.094(13)	2.059(13)
Ir(2)−C(4)	2.050(10)	2.048(14)	2.090(15)	2.078(13)
C(1)−O(1)	1.153(12)	1.159(11)	1.182(16)	1.192(16)
C(2)−O(2)	1.185(12)	1.165(11)	1.175(16)	1.161(16)
ϕ	89.0	89.5	89.0	89.7

[a] Bond lengths are given in Å; ϕ is the angle between the C(1)−Ir(1)−Ir(2)−C(2) and C(3)−Ir(1)−Ir(2)−C(4) planes, given in deg.

The molecule of **4** sits on a crystallographic inversion center, and the C_6F_4CN rings are also parallel but trans with respect to each other across the Ir−Ir bond. Unlike in **3** and **3a**, the CO ligands are in terminal positions. Interestingly, they are also oriented essentially perpendicular to the plane defined by the carbonyls and the iridium atoms ($\phi = 87.3°$). This mutually trans arrangement of the ligands is unique; the four known diiridium(II) complexes containing no bridging ligands that have been crystallographically studied have their ligands arranged in a staggered conformation,[6−9] and we believe that it can be traced to the HOMO-2 orbital, which was computed to have π-type symmetry, thus restricting rotation about the Ir−Ir bond (Figure 4). The Ir−Ir bond of **4** (2.8442(6) Å) is clearly longer than those in **3** (2.7655(5) and 2.7485(5) Å) and **3a** (2.7576(8) and 2.7583(8) Å). It is also longer than those of the other known diiridium(II) complexes containing no bridging ligands; the next closest is that found in the complex containing tetracyanobisimidazole ligands (2.826(2) Å).[9]

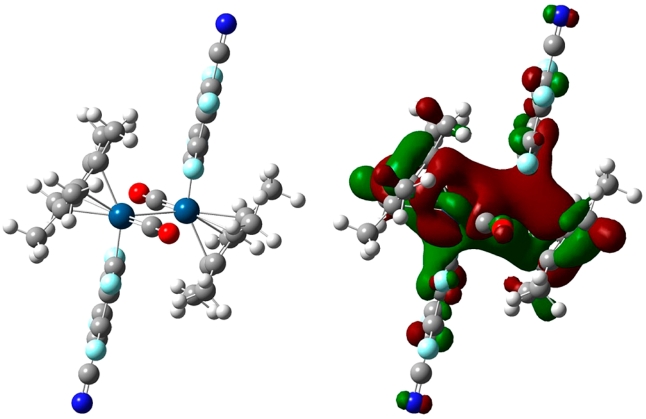

Figure 4. Computed molecular structures of **4** (left) and its HOMO-2 (right).

The ORTEP plot for **5** is shown in Figure 5, together with selected bond parameters. The molecule has a η^2-coordinated C_6F_6 ligand, and the associated bond parameters are similar to those of three other group 9 complexes containing such a moiety which have been structurally characterized: viz., $CpIr(C_2H_4)(\eta^2\text{-}C_6F_6)$ (**5a**),[18] $CpRh(PMe_3)(\eta^2\text{-}C_6F_6)$ (**5b**),[19] and $(\eta^5{:}\eta^1\text{-}C_5H_5SiMe_2CH_2PPh_2)Rh(\eta^2\text{-}C_6F_6)$ (**5c**).[20] An almost planar C_6F_4 unit is retained; the C(1)−C(2)−C(3)−C(3A) dihedral angle is only 1.4°, and F(2) and F(3) are bent out of the arene ring plane by 2.9 and 5.5°, respectively. The coordinated C═C bond (C(1)−C(1A) = 1.465(11) Å) is significantly lengthened compared to that of free C_6F_6 (1.394 Å), and the C−C bond lengths for the rest of the ring resemble those of a free diene, with a short (C(2)−C(3)), medium (C(3)−C(3A)), short (C(3A)−C(2A)) pattern, as observed for **5a**−**c**. The fluorine atoms (F(1) and F(1A)) on the carbon atoms bonded to the Ir atom bend strongly away from the plane of the aromatic ring; the dihedral angle between the C_6 ring plane and the F(1)−C(1)−C(1A)−F(1A) plane is 47.0°, similar to that reported for **5a** (47.9°) but larger than those for the Rh complexes (43.8 and 38.0°, for **5b**,**c**, respectively), and is probably a consequence of the larger size of Ir compared to Rh. Thus, the C_6F_6 ligand resembles a coordinated alkene in geometry.

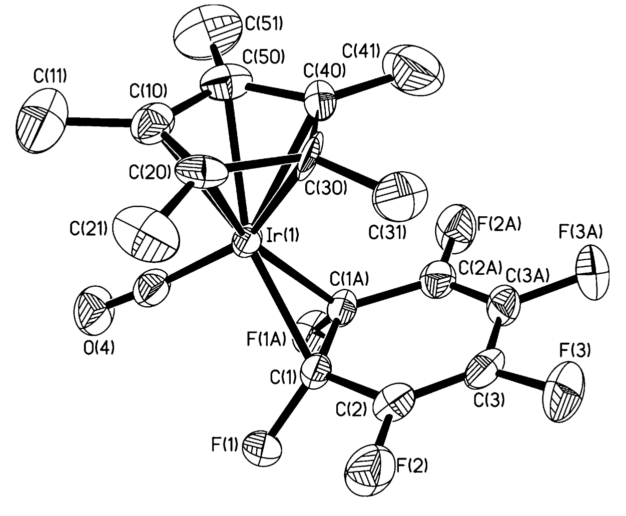

Figure 5. ORTEP plot showing the molecular structure of **5**, with thermal ellipsoids drawn at the 50% probability level. Hydrogen atoms have been omitted for clarity. Selected bond distances (Å) and angles (deg): Ir(1)−C(4) = 1.863(9); Ir(1)−C(1) = 2.071(6); C(4)−O(4) = 1.124(11); F(1)−C(1) = 1.390(6); F(2)−C(2) = 1.340(8); F(3)−C(3) = 1.351(7); C(1)−C(1A) = 1.465(11); C(1)−C(2) = 1.469(9); C(2)−C(3) = 1.317(10); C(3)−C(3A) = 1.428(13); C(1)−C(2)−C(3)−C(3A) = 1.4(6).

CONCLUDING REMARKS

We have reported here the unusual formation of two isomeric diiridium(II) complexes **3** and **4** from the visible light irradiation of $Cp^*Ir(CO)_2$ in pentafluorobenzonitrile; the generation of an analogue from hexafluorobenzene occurred less readily. Complex **4** is one of the few examples of such a species that does not contain a bridging ligand across the Ir−Ir bond, and it appears to be the less stable isomer. The reaction pathway is believed to proceed via initial nucleophilic attack on the aromatic ring followed by generation of an organometallic radical species **C**. Although the precise role of irradiation in the reaction remains unclear, it has a decided role in the isomerization of **4** to **3**, which is believed to proceed via **C** resulting from homolytic fission of the Ir−Ir bond. Complex **4**, and probably **3** as well, is therefore a ready precursor for the organometallic radical $[Cp^*Ir(CO)(C_6F_4CN)]^•$, and we are in the process of further exploration of its chemistry.

■ EXPERIMENTAL SECTION

General Procedures. All reactions and manipulations were performed under argon using standard Schlenk techniques unless stated otherwise. Visible light irradiation was carried out using a Phillips 60 W commercial light bulb. UV irradiation was carried out using a 450 W medium-pressure mercury lamp (peak emission at 254 nm). NMR spectra were recorded on a JEOL ECA400 or ECA400SL NMR spectrometer as $CDCl_3$ solutions unless otherwise stated; ^1H chemical shifts reported were referenced against the residual proton signals of the solvent. ^{19}F chemical shifts reported were referenced against external trifluoroacetic acid; designations of the F atoms are with respect to the iridium atom. Electrospray ionization (ESI) mass spectra were obtained on a Thermo Deca Max (LCMS) mass spectrometer with an ion-trap mass detector at 15 eV and 40 °C using direct injection of the sample. Fast atom bombardment (FAB) mass spectra were obtained on a Finnigan MAT95XL-T spectrometer in a 3NBA matrix (FAB). All elemental analyses were performed by the microanalytical laboratory at NUS. $Cp^*Ir(CO)_2$ (**1**)[21] and $Cp^*Ir(CO)(COOH)(C_6F_4CN)$ (**2**)[9] were prepared according to their published methods. All other reagents were from commercial sources and used without further purification.

Computational Studies. The reaction energetics for the reactions were studied by DFT theory utilizing Becke's three-parameter hybrid function[22] and Lee, Yang, and Parr's gradient-corrected correlation function (B3LYP).[23] The LANL2DZ (Los Alamos effective core potential double-ζ) basis set was employed for all atoms.[24] Excited state calculations were carried out with the TD method using the same basis set.[25] For calculations involving solvated species, the Onsager model was employed. The dielectric constant for the solvent C_6F_5CN was estimated as 21, on the basis of its polarity of 2.4 D in comparison to that of 2.9 D in acetone, which has a dielectric constant of 20.7. Harmonic frequencies were calculated at the optimized geometries to characterize stationary points as equilibrium structures with all real frequencies and to evaluate zero-point energy (ZPE) corrections. All calculations were performed using the Gaussian 09 suite of programs.[26]

Optimization of the structure of the solvated Meisenheimer zwitterion was first carried out in the gas phase to give a structure in which the C_6F_4CN ring was oriented parallel to the Cp* ring. The cavity radius (a_0) of this was used to optimize the zwitterion in the solvated phase to the structure depicted in Scheme 4. The cavity volume for this was then calculated and the new value of a_0 employed to reoptimize the structure.

Synthesis of $[Cp^*Ir(\mu\text{-}CO)(C_6F_4CN)]_2$ (3 and 4). In a Carius tube containing dried 4 Å molecular sieves (7 pieces), **1** (25 mg, 0.0653 mmol) and C_6F_5CN (0.25 mL, 0.383 g, 1.98 mmol) were added. The yellow solution was irradiated with a tungsten lamp and stirred slowly at room temperature for 24 h. A red suspension was formed. Volatiles were removed under reduced pressure, and the remaining red residue was resuspended in ether (10 mL). After collection of a reddish orange powder via filtration, it was washed with ether (5 mL) and dried under reduced pressure to yield spectroscopically pure **3**.

When the reaction was only carried out for 4 h, the terminal CO isomer $[Cp^*Ir(CO)(C_6F_4CN)]_2$ (**4**) was obtained together with **3** as a side product. X-ray diffraction quality crystals of **4** were grown from a dichloromethane/hexane solution of a mixture of **3** and **4** at room temperature.

Data for **3** are as follows. Yield (spectroscopic): ~90% to quantitative. IR ν_{CO} (CH_2Cl_2): 1770 (vs). ^1H NMR: δ 1.83 (s, 30H) ppm. ^{19}F NMR: δ −36.2 (m, 2F, F_{ortho}), −60.9 (m, 2F, F_{meta}) ppm. FAB-MS+ (m/z): 1058 [M], 1030 [M − CO], 530 [M/2], 502 [M/2 − CO]. Anal. Found: C, 40.68; H, 2.79; N, 2.74. Calcd: C, 40.83; H, 2.86; N, 2.65.

Data for **4** are as follows. Yield (spectroscopic): maximum ~50%. IR ν_{CO} (CH_2Cl_2): 2051 (vs). ^1H NMR: δ 1.49 (s, 30H) ppm. ^{19}F NMR: δ −34.5 (m, 2F, F_{ortho}), −59.9 (m, 2F, F_{meta}) ppm.

In an attempt to detect formation of oxalic acid via IR spectroscopy, three cycles of freeze−pump−thaw were performed on the crude reaction mixture at the end of the reaction. The Carius tube was then exposed to air and left to thaw. After the mixture thawed, volatiles were removed under reduced pressure, and the residue was extracted with ether. The ether extract was dried and an IR spectrum was collected using the KBr pellet method. No oxalic acid was observed.

A similar procedure was employed to monitor the ratio of **3** to **4** under varying irradiation times. After reaction for the designated number of hours, volatiles were removed under reduced pressure, and ^1H and ^{19}F NMR spectra were recorded.

Reaction of 1 with C_6F_5CN in the Dark. In a Carius tube containing dried 4 Å molecular sieves (7 pieces) was added **1** (10 mg, 0.026 mmol) and C_6F_5CN (0.25 mL, 0.383 g, 1.98 mmol). The reaction vessel containing the yellow solution was wrapped in aluminum foil and placed inside a wooden box, and the mixture was stirred slowly at room temperature for 24 h. An orange solution was formed. Volatiles were removed under reduced pressure, and a ^1H NMR spectrum of the remaining oil showed that **D** and **E** were obtained in a 5/2 ratio.

Data for **D** are as follows. IR ν_{CO} (hexane): 2019 cm^{-1}. ^1H NMR: δ 1.73 (s) ppm. ^{19}F NMR: δ −29.3 (m, 1F), −40.6 (m, 1F), −60.3 (m, 1F), −60.8 (m, 1F) ppm.

Data for **E** are as follows. IR ν_{CO} (hexane): 2002. ^1H NMR: δ 1.76 (s) ppm. ^{19}F NMR: δ −30.5 (m, 1F), −39.3 (m, 1F), −64.1 (m, 1F) ppm.

Photochemical Reaction of 1 and C_6F_6. In a quartz Carius tube containing **1** (20 mg, 0.0522 mmol) was added C_6F_6 (2 mL). The mixture was degassed by three cycles of freeze−pump−thaw and then irradiated for 20 h. An orange-brown solution was formed. Volatiles were removed under reduced pressure, and the remaining residue was extracted with cyclohexane (20 mL). The cyclohexane extract was dried in vacuo to give a brown-yellow oil (26.9 mg). The ^1H NMR spectrum of the oil showed the presence of **5** and **3a** (5/1 ratio by integration) and small amounts of unidentified products. Recrystallization from toluene and cyclopentane gave a larger proportion of **5** in the supernatant, but complete separation was not obtained. Prolonged irradiation led to slow precipitation of a tan solid containing a mixture of unidentified products.

X-ray diffraction quality crystals of **5** and **3a** were grown from a toluene/hexane solution of the mixture at 5 °C.

Data for **3a** are as follows. Yield (spectroscopic): ~15%. IR ν_{CO} (cyclohexane): 1778 (vs). ^1H NMR: δ 1.82 (s, 30H) ppm. ^{19}F NMR: δ −39.0 (m, 2F, F_{ortho}), −85.2 (t, 1F, F_{para}), −88.5 (m, 2F, F_{meta}) ppm. FAB-MS+ (m/z): 523 [M/2].

Data for **5** are as follows. Yield (spectroscopic): ~80%. Yield (isolated): 28%. IR ν_{CO} (cyclohexane): 2027 (vs). ^1H NMR: δ 1.89 (s, 15H) ppm. ^{19}F NMR: δ −71.4 (m, 2F, F^2 and F^{2A}), −77.9 (m, 2F, F^1 and F^{1A}), −97.9 (m, 2F, F^3 and F^{3A}) ppm. FAB-MS+ (m/z): 523 [M − F], 495 [M − F − CO], 356 [M − C_6F_6]. Anal. Found: C, 39.90; H, 3.13. Calcd for $C_{17}H_{15}F_6IrO\cdot{}^1/_4C_6H_{12}$: C, 39.50; H, 3.23.

Reaction of 3 with Chloroform. In a Carius tube containing **3** (10 mg, 0.0095 mmol) was added $CHCl_3$ (1 mL). The red solution was irradiated for 12 h under a tungsten lamp, with stirring. A yellow solution was formed within 4 h. Volatiles were removed under reduced pressure, and a ^1H NMR spectrum showed quantitative conversion to $Cp^*Ir(CO)(C_6F_4CN)(Cl)$ (**6**). The same observations could be made when an NMR sample of **3** was left in $CDCl_3$ for a few hours. The product could be purified by TLC with dichloromethane/hexane (2/1, v/v) as the eluent. When the reaction was performed in the dark, no reaction occurred.

Data for **6** are as follows. IR ν_{CO} (CH_2Cl_2): 2053 (vs). ^1H NMR: δ 1.94 (s, 15H) ppm. ^{19}F NMR: δ −35.1 (s, br, 2F, F_{ortho}), −58.8 (m, 2F, F_{meta}) ppm. FAB-MS+ (m/z): 538 [M − CO + H], 530 [M − Cl]. HR-FAB: calcd for $C_{18}H_{15}F_4NO^{193}Ir$ ([M − Cl]) 530.0714, found 530.0697.

Crystal Structure Determinations. Crystals were mounted on quartz fibers. X-ray data were collected on a Bruker AXS APEX system, using Mo Kα radiation, with the SMART suite of programs.[27] Data were processed and corrected for Lorentz and polarization effects with SAINT[28] and for absorption effects with SADABS.[29] Structural solution and refinement were carried out with the SHELXTL suite of programs.[30] The structures were solved by direct methods to locate the heavy atoms, followed by difference maps for the light, non-hydrogen atoms. Organic hydrogen atoms were placed in calculated positions and refined with a riding model. All non-hydrogen atoms were given anisotropic displacement parameters in the final model. The crystal of **3a** contained a disordered hexane solvate. This was modeled with two alternative sites of equal occupancies (0.25), with all the carbon atoms assigned a common isotropic thermal parameter and appropriate bond restraints applied. The molecule of **5** was located across a crystallographic mirror plane and exhibited disorder of the Cp* ring about this plane.

■ ASSOCIATED CONTENT

Ⓢ Supporting Information

Tables, figures, and CIF files giving additional characterization data, crystallographic data for **3**, **3a**, **4**, and **5**, and computed structures. This material is available free of charge via the Internet at http://pubs.acs.org.

■ AUTHOR INFORMATION

Notes

The authors declare no competing financial interest.

■ ACKNOWLEDGMENTS

This work was supported by an A*STAR grant (Research Grant No. 012 101 0035). K.H.G.M. thanks the National University of Singapore for Research Scholarships.

■ REFERENCES

(1) Ebihara, M.; Kanematsu, N.; Sakuma, T.; Noritake, S.; Kawamura, T. *Inorg. Chem. Acta* **2005**, *358*, 2174.

(2) Casado, M. A.; Perez-Torrente, J. J.; Ciriano, M. A.; Dobrinovitch, I. T.; Lahoz, F. J.; Oro, L. A. *Inorg. Chem.* **2003**, *42*, 3956.

(3) Kimura, T.; Ishiwata, K.; Kuwata, S.; Ikariya, T. *Organometallics* **2012**, *31*, 1204.

(4) Tejel, C.; Ciriano, M. A.; López, J. A.; Lahoz, F. J.; Oro, L. A. *Organometallics* **2000**, *19*, 4977.

(5) Del Rossi, K. J.; Wayland, B. B. *J. Chem. Soc., Chem. Commun.* **1986**, 1653.

(6) Hückstädt, H.; Homborh, H. *Z. Anorg. Allg. Chem.* **1997**, *623*, 369.

(7) Rasmussen, P. G.; Anderson, J. E.; Bailey, O. H.; Tamres, M.; Bayón, J. C. *J. Am. Chem. Soc.* **1985**, *107*, 279.

(8) Patra, S. K.; Rahaman, S. M. W.; Majumdar, M.; Sinha, A.; Bera, J. K. *Chem. Commun.* **2008**, 2511.

(9) Heinekey, D. M.; Fine, D. A.; Barnhart, D. *Organometallics* **1997**, *16*, 2530.

(10) Chan, P. K.; Leong, W. K. *Organometallics* **2008**, *27*, 1247.

(11) (a) Jiang, F.; Biradha, K.; Leong, W. K.; Pomeroy, R. K. *Can. J. Chem.* **1999**, *77*, 1327. (b) Einstein, F. W. B.; Pomeroy, R. K.; Rushman, P.; Willis, A. C. *Organometallics* **1985**, *4*, 250.

(12) Burdeniuc, J.; Jedlicka, B.; Crabtree, R. H. *Chem. Ber.* **1997**, *130*, 145.

(13) Hoyano, J. K.; Graham, W. A. G. *J. Am. Chem. Soc.* **1982**, *104*, 3723.

(14) Hoyano, J. K.; McMaster, A. D.; Graham, W. A. G. *J. Am. Chem. Soc.* **1983**, *105*, 7190.

(15) Jobling, M.; Howdle, S. M.; Poliakoff, M. *J. Chem. Soc. Chem. Comm.* **1990**, *24*, 1762.

(16) (a) Hicks, C.; Fan, J.; Rutenberg, I.; Gafney, H. D. *Coord. Chem. Rev.* **1998**, *171*, 71. (b) Fox, M. A. *Chem. Rev.* **1979**, *79*, 253.

(17) (a) Ebsworth, E. A. V.; Robertson, N.; Yellowlees, L. J. *J. Chem. Soc., Dalton Trans.* **1993**, 1031. (b) Blake, A. J.; Cockman, R. W.; Ebsworth, E. A. V.; Holloway, J. H. *J. Chem. Soc., Chem. Commun.* **1988**, 529.

(18) Bell, T. W.; Helliwell, M.; Partridge, M. G.; Perutz, R. N. *Organometallics* **1992**, *11*, 1911.

(19) (a) Belt, S. T.; Duckett, S. B.; Helliwell, M.; Perutz, R. N. *J. Chem. Soc., Chem. Commun.* **1989**, 928−930. (b) Belt, S. T.; Helliwell, M.; Jones, W. D.; Partridge, M. G.; Perutz, R. N. *J. Am. Chem. Soc.* **1993**, *115*, 1429−1440.

(20) Lefort, L.; Crane, T. W.; Farwell, M. D.; Baruch, D. M.; Kaeuper, J. A.; Lachicotte, R. J.; Jones, W. D. *Organometallics* **1998**, *17*, 3889.

(21) Ball, R. G.; Graham, A. G.; Heinekey, D. M.; Hoyano, J. K.; McMaster, A. D.; Mattson, B. M.; Michel, S. T. *Inorg. Chem.* **1990**, *29*, 2023.

(22) Becke, A. D. *J. Chem. Phys.* **1993**, *98*, 5648.

(23) Lee, C.; Yang, W.; Parr, R. G. *Phys. Rev. B* **1998**, *37*, 785.

(24) Ehlers, A. W.; Böhme, M.; Dapprich, S.; Gobbi, A.; Höllwarth, A.; Jonas, V.; Köhler, K. F.; Stegmann, R.; Veldkamp, A.; Frenking, G. *Chem. Phys. Lett.* **1993**, *208*, 111.

(25) Foresman, J. B.; Head-Gordon, M.; Pople, J. A.; Frisch, M. J. *J. Phys. Chem.* **1992**, *109*, 8218.

(26) Frisch, M. J.; Trucks, G. W.; Schlegel, H. B.; Scuseria, G. E.; Robb, M. A.; Cheeseman, J. R.; Scalmani, G.; Barone, V.; Mennucci, B.; Petersson, G. A.; Nakatsuji, H.; Caricato, M.; Li, X.; Hratchian, H. P.; Izmaylov, A. F.; Bloino, J.; Zheng, G.; Sonnenberg, J. L.; Hada, M.; Ehara, M.; Toyota, K.; Fukuda, R.; Hasegawa, J.; Ishida, M.; Nakajima, T.; Honda, Y.; Kitao, O.; Nakai, H.; Vreven, T.; Montgomery, J. A., Jr.; Peralta, J. E.; Ogliaro, F.; Bearpark, M.; Heyd, J. J.; Brothers, E.; Kudin, K. N.; Staroverov, V. N.; Kobayashi, R.; Normand, J.; Raghavachari, K.; Rendell, A.; Burant, J. C.; Iyengar, S. S.; Tomasi, J.; Cossi, M.; Rega, N.; Millam, J. M.; Klene, M.; Knox, J. E.; Cross, J. B.; Bakken, V.; Adamo, C.; Jaramillo, J.; Gomperts, R.; Stratmann, R. E.; Yazyev, O.; Austin, A. J.; Cammi, R.; Pomelli, C.; Ochterski, J. W.; Martin, R. L.; Morokuma, K.; Zakrzewski, V. G.; Voth, G. A.; Salvador, P.; Dannenberg, J. J.; Dapprich, S.; Daniels, A. D.; Farkas, Ö.; Foresman, J. B.; Ortiz, J. V.; Cioslowski, J.; Fox, D. J. *Gaussian 09*; Gaussian Inc., Wallingford, CT, 2009.

(27) *SMART version 5.628*; Bruker AXS Inc., Madison, WI, 2001.

(28) *SAINT+ version 6.22a*; Bruker AXS Inc., Madison, WI, 2001.

(29) Sheldrick, G. M. *SADABS*; 1996.

(30) *SHELXTL version 5.1*; Bruker AXS Inc., Madison, WI, 1997.